Crankshaft Motion in a Highly Congested Bis(triarylmethyl)peroxide

Tinh-Alfredo V. Khuong,[†] Gerardo Zepeda,[‡] Carlos N. Sanrame,[†] Hung Dang,[†]
Michael D. Bartberger,[†] K. N. Houk,[†] and Miguel A. Garcia-Garibay*,[†]

*Contribution from the Department of Chemistry and Biochemistry, University of California,
Los Angeles, 405 Hilgard Avenue, Los Angeles, California 90095-1569, and
Departamento de Quimica Organica, Escuela Nacional de Ciencias Biologicas, IPN,
Prol. Carpio y Plan de Ayala, 11340, Mexico*

Received May 21, 2004; E-mail: mgg@chem.ucla.edu

Abstract: Crankshaft motion has been proposed in the solid state for molecular fragments consisting of
three or more rotors linked by single bonds, whereby the two terminal rotors are static and the internal
rotors experience circular motion. Bis-[tri-(3,5-di-*tert*-butyl)phenylmethyl]-peroxide **2** was tested as a model
in search of crankshaft motion at the molecular level. In the case of peroxide **2**, the bulky trityl groups may
be viewed as the external static rotors, while the two peroxide oxygens can undergo the sought after internal
rotation. Evidence for this process in the case of peroxide **2** was obtained from conformational dynamics
determined by variable-temperature ^{13}C and ^{1}H NMR between 190 and 375 K in toluene-d_8. Detailed spectral
assignments for the interpretation of two coalescence processes were based on a correlation between
NMR spectra obtained in solution at low temperature, in the solid state by ^{13}C CPMAS NMR, and by GIAO
calculations based on a B3LYP/6-31G** structure of **2** obtained from its X-ray coordinates as the input.
Evidence supporting crankshaft rotation rather than slippage of the trityl groups was obtained from molecular
mechanics calculations.

Introduction

In recent years, chemists have recognized analogies between the dynamic behavior of molecules and the function of simple machines and machine parts.[1−3] Examples reported in the literature include molecular propellers,[4] gears,[5] turnstiles,[6] and ratchets,[7] among many others. Although it is unlikely that any one of those "artificial molecular machines" will find applica-

tions analogous to those of their macroscopic namesakes, the suggested resemblances stimulate a deeper understanding of molecular kinematics[8] and challenge organic chemists to synthesize molecules that may conform to desired dynamic behaviors. In this context, we recently became interested in identifying conformational processes that are likely to occur in the solid state and other rigid media.[9] On the basis of the topochemical postulate,[10] we reasoned that shape- and volume-conserving motions should be the best candidates, and we have confirmed this hypothesis with compounds that emulate macroscopic compasses and gyroscopes. We have shown that axially substituted diethynyl benzenes can undergo rotations with rate constants greater than 10^8 s^{-1} in the solid state,[10,11] and, as an extension of that work, we have investigated structures with groups that might undergo circular displacements analogous to those encountered in macroscopic crankshafts.

† University of California, Los Angeles.

‡ Escuela Nacional de Ciencias Biologicas.

(1) For pioneering thoughts on artificial molecular machines, see: Mislow, K. *Chemtracts: Org. Chem.* **1988**, *2*, 151−174.

(2) (a) Sauvage, J.-P., Ed. *Molecular Machines and Motors*; Springer-Verlag: New York, 2001; p 99. (b) Balzani, V.; Credi, A.; Raymo, F. M.; Stoddart, J. F. *Angew. Chem., Int. Ed.* **2000**, *39*, 3348−3391.

(3) Special Issue on Molecular Machines. *Acc. Chem. Res.* **2001**, *34*. (a) Shinkai, S.; Ikeda, M.; Sugasaki, A.; Takeuchi, M. *Acc. Chem. Res.* **2001**, *34*, 494−503. (b) Stoddart, J. F. *Acc. Chem. Res.* **2001**, *34*, 410−411. (c) Bustamante, C.; Keller, D.; Oster, G. *Acc. Chem. Res.* **2001**, *34*, 412−420. (d) Shipway, A. N.; Willner, I. *Acc. Chem. Res.* **2001**, *34*, 421−432. (e) Pease, A. R.; Jeppesen, J. O.; Stoddart, J. F.; Luo, Y.; Collier, C. P.; Heath, J. R. *Acc. Chem. Res.* **2001**, *34*, 433−444. (f) Ballardini, R.; Balzani, V.; Credi, A.; Gandolfi, M. T.; Venturi, M. *Acc. Chem. Res.* **2001**, *34*, 445−455. (g) Harada, A. *Acc. Chem. Res.* **2001**, *34*, 456−464. (h) Schalley, C. A.; Beizai, K.; Vögtle, F. *Acc. Chem. Res.* **2001**, *34*, 465−476. (i) Collin, J.-P.; Dietrich-Buchecker, C.; Gaviña, P.; Jimenez-Molero, M. C.; Sauvage, J.-P. *Acc. Chem. Res.* **2001**, *34*, 477−487. (j) Amendola, L.; Fabbrizzi, C.; Mangano, P.; Pallavicini. *Acc. Chem. Res.* **2001**, *34*, 488−493. (k) Feringa, B. L. *Acc. Chem. Res.* **2001**, *34*, 504−513. (l) Kelly, T. R. *Acc. Chem. Res.* **2001**, *34*, 514−522.

(4) (a) Mislow, K. *Acc. Chem. Res.* **1976**, *9*, 26−33. (b) Mislow, K.; Gust, D.; Finocchiaro, P.; Boettcher, R. J. *Top. Curr. Chem.* **1974**, *47*, 1−28. (c) Finocchiaro, P.; Gust, D.; Hounshell, W. D.; Hummel, J. P.; Maravigna, P.; Mislow, K. *J. Am. Chem. Soc.* **1976**, *98*, 4945−4952.

(5) (a) Hounshell, W. D.; Johnson, C. A.; Guenzi, A.; Cozzi, F.; Mislow, K. *Proc. Natl. Acad. Sci. U.S.A.* **1980**, *77*, 6961−6964. (b) Iwamura, I.; Mislow, K. *Acc. Chem. Res.* **1988**, *21*, 175−182. (c) Oki, M. *The Chemistry of Rotational Isomers*; Springer-Verlag: Berlin, 1993.

(6) Bedard, T. C.; Moore, J. *J. Am. Chem. Soc.* **1995**, *117*, 10662−10671.

(7) (a) Kelly, T. R.; Tellitu, I.; Sestelo, J. P. *J. Org. Chem.* **1997**, *63*, 3655−3665. (b) Kelly, T. R.; Tellitu, I.; Sestelo, J. P. *Angew. Chem., Int. Ed. Engl.* **1997**, *36*, 1866−1868.

(8) Kinematics is a branch of physics concerned with describing the motion of objects with respect to suitable coordinate systems. The causes of that motion are addressed by dynamics.

(9) (a) Dominguez, Z.; Dang, H.; Strouse, M. J.; Garcia-Garibay, M. A. *J. Am. Chem. Soc.* **2002**, *124*, 2398−2399. (b) Dominguez, Z.; Dang, H.; Strouse, M. J.; Garcia-Garibay, M. A. *J. Am. Chem. Soc.* **2002**, *124*, 7719−7727. (c) Godinez, C. E.; Zepeda, G.; Garcia-Garibay, M. A. *J. Am. Chem. Soc.* **2002**, *124*, 4701−4707.

(10) The topochemical postulate was formulated by Kohlshutter as an indication of the type of atomic and molecular displacements that may be observable in crystals within the context of chemical reactivity. The same constraints will apply to conformational motions, which may be also considered elementary chemical process. Kohlshutter, H. W. *Anorg. Allg. Chem.* **1918**, *105*, 121.

(11) Khuong, T.-A. V.; Zepeda, G.; Ruiz, R.; Kahn, S. I.; Garcia-Garibay, M. A. *Cryst. Growth Des.* **2003**, *5*, 15−18.
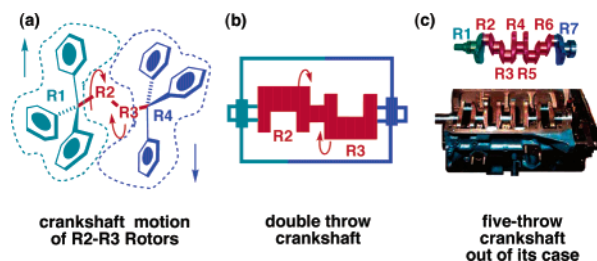
Figure 1. Analogy between bis(triarylmethyl) derivative (a) and a double throw crankshaft (b). A five-throw crankshaft is also shown (c) to clarify the suggested analogy. In a reciprocating engine, the rotary motion of a crankshaft shaft −R2−Rn−1− couples to the up-and-down motion of the pistons (not shown in the figure). The arrows in (a) indicate how the up-and-down motions of the trityl groups may lead to the circular motion of −R2−R3−.

Scheme 1

A macroscopic crankshaft is a machine part that interconverts "to-and-fro" into rotary motion.[12] Crankshaft motion in chemistry has been postulated to explain the relaxation processes of certain polymers in terms of the correlated dynamics of three or more rotors linked by single bonds.[13] These rotors may be methylene, ethylene, or aromatic groups, as well as more complex substructures.[14] Crankshaft motion occurs when the end-rotors (R1 and Rn) remain stationary relative to each other, while the central ones (R2, R3..., Rn−1) undergo circular motion. While crankshaft motion in solids should be unambiguously described by a macroscopic frame of reference given by the bulk material, crankshaft motion for rapidly tumbling molecules in solution must be defined from an internal frame of reference. In this paper, we investigate the potential crankshaft motion of a molecule with four rotors consisting of two triarylmethyl (trityl) end groups (R1 and R4) that are linked through their methane carbons by a short peroxide tether, −R2−R3−, as illustrated in Figure 1a. Ideally, the two bulky bis-(triarylmethyl) derivatives will be tightly meshed and unable to rotate (slip) past each other, providing a relatively rigid frame of reference where the suggested crankshaft motion will be emulated by the −R2−R3− groups, as represented in Figure 1. Although we hypothesize that a molecular crankshaft designed to function in solution may be fine-tuned to function in the solid state, in this paper we will center on solution studies: we will (a) formulate the requirements for the experimental characterization of the crankshaft motion, (b) describe variable-temperature NMR results with bis-[3,5-di-*tert*-butyl-triphenylmethyl]-peroxide **2** (Scheme 1), (c) assign the low-temperature ^{1}H and ^{13}C NMR spectra by a correlation of experimental and computational results, (d) provide strong evidence for those assignments, (e) use the latter assignments to carry out detailed line-shape simulations in support of a crankshaft process, and (f) explore "crankshaft" and "slippage" trajectories to help explain the experimental data.

Results and Discussion

A Molecular Crankshaft: Conceptualization and Design.
While many molecular and supramolecular assemblies having
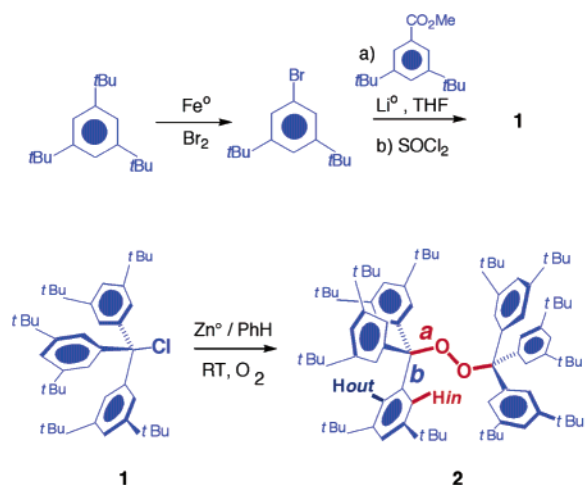
two rigid ends linked to internal rotors may be conceived, we envision a very simple conceptualization of a crankshaft with compounds having two trityl groups (fixed rotors R1− and −R4) linked through their methane carbons by a two atom tether, −R2−R3−, as illustrated in Figure 1a.

The selection of a test model to document the sought after crankshaft motion by variable-temperature NMR (VT-NMR) must consider all of the (residual) isomers[15] that can be detected under the conditions of the experiment, and a strategy to assign experimental observables in terms of the postulated motion. Ideally, the only residual isomers in the system should be those related by the dynamics of the desired process, in this case, those isomers related by the circular motion of the −A−B− groups. Fortunately, the stereochemistry and stereodynamics of trityl derivatives have been extensively investigated, greatly facilitating the design of a suitable compound. It has been shown that asymmetric trityl groups may have as many as 32 stereoisomers (2^5), resulting from one chiral center at the methane carbon, one chiral axis that results in two propeller conformations, and one chiral plane for each of the aromatic groups with nonequivalent rotamers. Given that structures with two trityl groups may have as many as 2^{10} stereoisomers, it seemed essential to design compounds with the lowest possible structural complexity. Therefore, on the basis of symmetry considerations, steric bulk, and ease of preparation, we selected bis-[tri-(3,5-di-*tert*-butyl)phenylmethyl]-peroxide **2**[16] as a test compound (Scheme 1). It is worth noting that compound **2** can only exist as a chiral D,L-pair or as a meso isomer, which result from the axial chirality of the two trityl groups.

Synthesis and X-ray Structure. Peroxide **2** is a known compound obtained by addition of O_2 to the trityl radical generated from tris-(3,5-di-*tert*-butylphenyl)methyl chloride **1** (Scheme 1). Trityl chloride **1** was prepared from commercially available 1,3,5-tri-*tert*-butylbenzene and methyl-3,5-di-*tert*-butylbenzoate by reported procedures.[17,18] As expected for a conformationally hindered system, the ^{1}H and ^{13}C NMR spectra

(12) Datsko, J. *Encyclopedia Americana Online*; Grolier, Inc.; To be found under http://ea.grolier.com, 1999.
(13) Moro, G. T. *J. Phys. Chem.* **1996**, *100*, 16419−16422.
(14) (a) David, L.; Girard, C.; Dolmazon, R.; Albrand, M.; Etienne, S. *Macromolecules* **1996**, *29*, 8343−8348. (b) Hikmet, R. A. M.; Broer, D. J. P. *Polymer* **1991**, *32*, 1627−1632. (c) Gurler, M. T.; Crabb, C. C.; Dahlin, D. M.; Kovac, J. *Macromolecules* **1983**, *16*, 398−403. (d) Boyd, R. H.; Breitling, S. M. *Macromolecules* **1974**, *7*, 855−862. (e) Jones, A. A.; Stockmayer, W. H. *J. Polym. Sci., Polym. Phys. Ed.* **1977**, *15*, 847−861.

(15) Eliel, E. L.; Wilen, S. H. *Stereochemistry of Organic Compounds*; John Wiley & Sons: New York, 1994.
(16) (a) Kahr, B.; Van Engen, D.; Mislow, K. *J. Am. Chem. Soc.* **1986**, *108*, 8305−8307. (b) Schreiner, K.; Berndt, A.; Baer, F. *Mol. Phys.* **1973**, *26*, 929−939.
(17) Bartlett, P. D.; Roha, M.; Stiles, M. *J. Am. Chem. Soc.* **1954**, *76*, 2349−2353
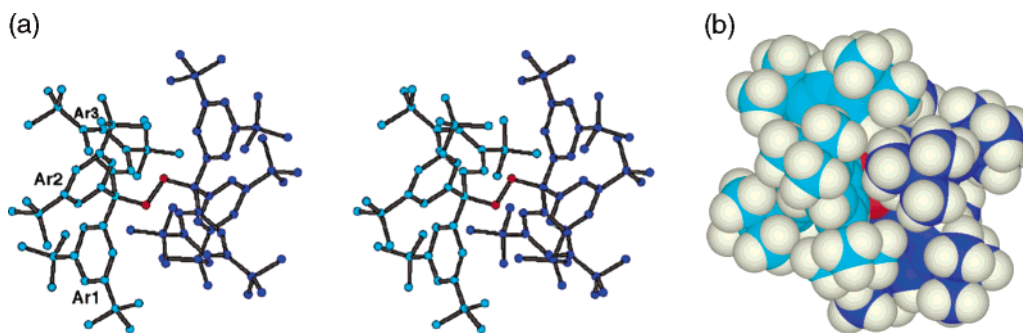(18) Pearce, P. J.; Richards, D. H.; Scilly, N. F. *J. Chem. Soc., Perkin Trans. 1* **1972**, 1655−1660.

Figure 2. (a) Stereoview of the X-ray meso (*C_i*) structure of peroxide **2** with hydrogen atoms omitted for clarity. Two color tones are used to illustrate the two trityl groups. The nonequivalent aromatic groups are labeled Ar1−Ar3. (b) Space-filling model illustrating the tight meshing of the two triarylmethyl groups.

of **2** revealed a strong temperature dependence which will be described in the following section. Good quality crystals of peroxide **2** were obtained from chloroform as colorless prisms, which are stable for months at ambient temperatures but decompose upon melting at 253 °C to give the 3,3′,5,5′-tetra-*tert*-butylbenzophenone as the main product. The crystal structure of peroxide **2** was solved by single-crystal X-ray diffraction analysis in the triclinic space group *P1̄* with two half molecules (A and B) per asymmetric unit which differ only by the degree of rotational disorder in one of the *tert*-butyl groups of one of them (molecule B).[19] As required by the space group symmetry, the two molecules of peroxide **2** adopt a centrosymmetric (*C_i*) meso form[20] with the two trityl groups adopting opposite axial chirality (Figure 2a). A crystallographic information file with detailed acquisition and refinement parameters is available in the Supporting Information.

The structural features of the peroxide group in **2** are similar to those of bis(triphenylmethyl)peroxide.[21] They include a C(quat)−O−O−C(quat) dihedral angle of 180°, and C(quat)−O and O−O distances of 1.474 and 1.461 Å, respectively. Given the crystallographic and magnetic nonequivalence of the three aromatic groups, it was considered useful to label them as Ar1, Ar2, and Ar3 (Figure 2a). The identities of the tree rings were defined by the dihedral angles formed between the plane of the aromatic rings and the C(quat)−O bond vector, or aryl "flip" angle (see below), and by the orientation of each ring (anti, +gauche, or −gauche) with respect to the O−O peroxide bond. The corresponding "flip" and "orientation" angles are 44.2° and 176.2°, respectively, for Ar1, 33.2° and −59.5° for Ar2, and 66.3° and 65.5° for Ar3. The space-filling model shown in Figure 2b illustrates the very dense molecular structure with aryl groups tightly interwoven across a plane perpendicular to the axis formed by a vector between the two trityl carbons.

Variable-Temperature ^{1}H NMR Spectroscopy. Although there are no contacts shorter than the sum of the van der Waals radii between hydrogen atoms in aryl groups at the two halves of **2**, space-filling models indicate that rotation of the two trityl groups past each other should be an activated process. VT ^{1}H NMR studies of compound **2** in toluene-*d_8* between 193 and 375 K revealed complex dynamics with two coalescence processes. The aromatic region between 6.4 and 8.4 shown in
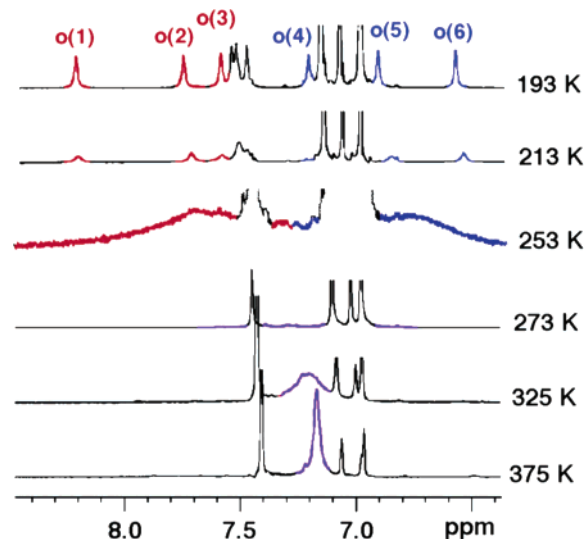
(19) The crystal structure of **2** consists of two-half molecules A and B, per asymmetric unit, which differ only by the rotational disorder of one *tert*-butyl group in B. Please see the Supporting Information.
(20) Crystals of **2** melt with decomposition at 253 °C, giving a sharp exothermic transition with a Δ*H* = −68 kcal/mol.
(21) Glidewell, C.; Liles, D. C.; Walton, D. J.; Sheldrick G. M. *Acta Crystallogr.* **1979**, *B35*, 500−502.

Figure 3. Aromatic region of variable-temperature 500 MHz ^{1}H NMR spectra of peroxide **2** in toluene-*d_8*. Solvent signals have been truncated for clarity.

Figure 3 was the most diagnostic. Time-averaged signals expected from fast trityl and aryl group rotation required temperatures as high as 375 K. Narrowing singlets were observed for the *ortho*- and *para*-hydrogens at 7.18 and 7.42 ppm, respectively (Figure 3, bottom spectrum). A decrease in temperature resulted in substantial broadening of the *ortho*-signal, which by 253 K had separated into two broad peaks centered at 6.75 and 7.70 ppm with a half-width at half-height of ca. 210 Hz. Further cooling resulted in additional splitting of each *ortho*-signal into three nonequivalent hydrogens, giving rise to six well-resolved peaks between 8.25 and 6.60 ppm (labeled o(1)−o(6) in Figure 3). A dispersion of 1.65 ppm can be assigned to the anisotropic field effects of aromatic and peroxy groups, which arise from the frozen rotation about peroxide−methyl and methyl−aryl bonds, labeled "a" and "b", respectively, in Scheme 1. The *para*-hydrogens also resolved at low temperature into three singlets at 7.48, 7.50, and 7.52 ppm, which are also illustrated in the top spectrum in Figure 3. While analogous measurements carried out in CDCl_3 between 213 and 232 K were consistent with those obtained in the aromatic solvent, we centered our attention on the latter based on the large temperature range of its liquid phase.
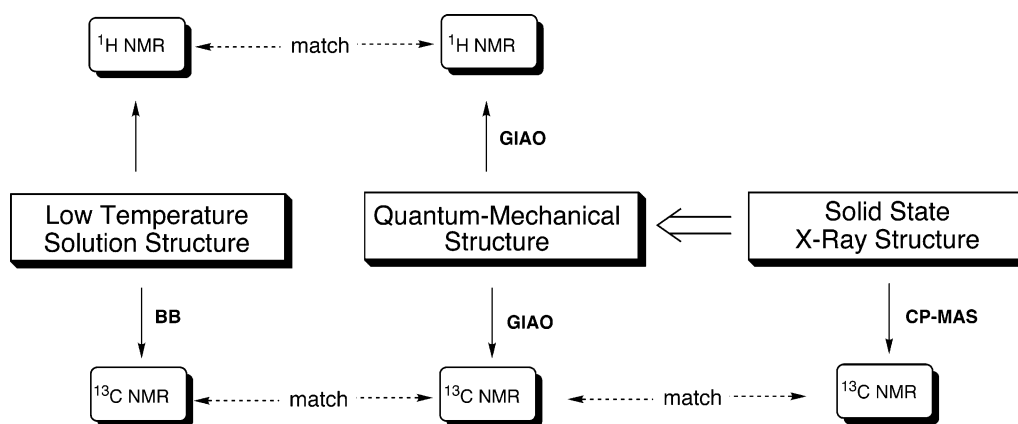
To pinpoint the coalescence behavior of **2** in terms of a mechanical model, one must establish the solution structure with a detailed assignment of all of the signals in Figure 3. The

Scheme 2

number of signals in the low-temperature spectrum is consistent with the C_i symmetry of the crystal structure. Nine aromatic signals arise from the one *para*- and two *ortho*-hydrogens on each of the three magnetically different aryl groups. Geometry minimizations with molecular mechanics (MM+) and semi-empirical methods (AM1) gave two energy minima consistent with the centrosymmetric (C_i) X-ray structure and a chiral isomer that deviates from C_2 symmetry to an asymmetric C_1 structure. Although the C_i and C_1 structures are nearly iso-energetic by molecular mechanics,[22] AM1 and single point B3LYP/6-31G*//MM+ DFT calculations favored the C_i isomer by 3.0 and 2.5 kcal/mol, respectively. In agreement with the quantum mechanical results, the low-temperature ^{1}H NMR spectrum of **2** is consistent with a single isomer, and all attempts to detect the second diastereomer by equilibration, and through heating and fast cooling cycles, were unsuccessful.

Assignment of the Low-Temperature Solution Spectrum by a Correlation of Experimental and Computational Results. While the large chemical shift dispersion of the aromatic *ortho*-hydrogens observed at low temperatures in peroxide **2** bodes well for a dynamic analysis, the formulation of a detailed mechanism based on site-exchange processes requires a precise assignment of all of the hydrogen resonances. Thus, knowing that most neutral molecules crystallize in their lowest energy conformations,[23] and with various examples of derivatives known to have comparable solution and solid-state structures,[24] we set out to search for a possible correlation between the structure present in solution and the structure determined by X-ray diffraction in the solid state. As illustrated in Scheme 2, our strategy relied on the possible correspondence between spectra acquired in solution and in the solid state with spectra calculated by the GIAO (gauge independent atomic orbitals) method from a quantum mechanical structure derived from the X-ray coordinates of **2**. In practical terms, a three-way correlation is only possible using ^{13}C NMR spectroscopy. While liquidlike ^{13}C NMR spectra may be obtained by cross polarization and magic angle spinning (CPMAS),[25] ^{1}H NMR spectroscopy in solids does not provide the necessary resolution to attempt a correlation of the isotropic chemical shift of the

aromatic signals. Despite this limitation, a good match between the three ^{13}C NMR spectra should be a strong indication of structural identity, suggesting a similarly good agreement within the calculated and observed ^{1}H frequencies. The spectrum of peroxide **2** was also calculated for the structure of the chiral C_1 isomer.

The results from ^{13}C NMR spectra obtained in CDCl$_3$ at 190 K, in the solid state at 300 K by ^{13}C CPMAS, and from the GIAO calculation are shown in Figures 4−6.[26] The ^{13}C CPMAS NMR spectrum was acquired with powdered crystals confirmed to be the same phase as that previously used to collect the X-ray data. The size of structure **2** imposed some limitations on the GIAO calculations which had to be carried out on models with the *tert*-butyl groups replaced with hydrogen atoms.[27] The model C_i structure was derived from the X-ray coordinates of **2** minimized with the B3LYP/6-31G* method. A model of the C_1 isomer was similarly derived from the B3LYP/6-31G*/MM+ structure previously found to be a higher energy diastereomer of **2**. Isotropic chemical shifts for both models were calculated in parts per million for each atom for both meso (C_i) and chiral (C_1) structures using the B3LYP density functional with a 6-31G** basis set. Graphical summaries of the experimental and computational results for the aromatic ^{1}H and ^{13}C resonances are illustrated in a bar graph format in Figures 4 and 5, respectively, with the calculated chemical shifts normalized to the upfield experimental signals.

To analyze the NMR results in Figures 4 and 5, the potential consequences of removing the *tert*-butyl group should be considered. Although field effects cannot be predicted without a GIAO calculation of the complete structure, the chemical shift dispersion of the aromatic ^{1}H and ^{13}C signals in solution is greater for the *tert*-butyl-substituted compound as compared to

(22) Molecular mechanics minimizations were carried out with the MM+ force field and the AM1 method as implemented by the Hyperchem Package: Hypercube, Inc., Gainsville, FL.

(23) Dunitz, J. D. *X-ray Analysis and the Structure of Organic Molecules*; Cornel University Press: Ithaca, NY, 1979.

(24) (a) Sabacky, M. J.; Johnson, S. M.; Martin, J. C.; Paul, I. C. *J. Am. Chem. Soc.* **1969**, *91*, 7542−7544. (b) Blount, J. F.; Finocchiaro, P.; Gust, D.; Mislow, K. *J. Am. Chem. Soc.* **1973**, *95*, 7019.

(25) (a) Fyfe, C. A. *Solid State NMR for Chemists*; C.F.C. Press: Guelph, Ontario, 1983. (b) Stejskal, E. O.; Memory, J. D. *High-Resolution NMR in the Solid State. Fundamentals of CP/MAS*; Oxford University Press: New York, 1994.

(26) DFT and GIAO calculations were performed with Gaussian 98: Frisch, M. J.; Trucks, G. W.; Schlegel, H. B.; Scuseria, G. E.; Robb, M. A.; Cheeseman, J. R.; Zakrzewski, V. G.; Montgomery, J. A., Jr.; Stratmann, R. E.; Burant, J. C.; Dapprich, S.; Millam, J. M.; Daniels, A. D.; Kudin, K. N.; Strain, M. C.; Farkas, O.; Tomasi, J.; Barone, V.; Cossi, M.; Cammi, R.; Mennucci, B.; Pomelli, C.; Adamo, C.; Clifford, S.; Ochterski, J.; Petersson, G. A.; Ayala, P. Y.; Cui, Q.; Morokuma, K.; Malick, D. K.; Rabuck, A. D.; Raghavachari, K.; Foresman, J. B.; Cioslowski, J.; Ortiz, J. V.; Stefanov, B. B.; Liu, G.; Liashenko, A.; Piskorz, P.; Komaromi, I.; Gomperts, R.; Martin, R. L.; Fox, D. J.; Keith, T.; Al-Laham, M. A.; Peng, C. Y.; Nanayakkara, A.; Gonzalez, C.; Challacombe, M.; Gill, P. M. W.; Johnson, B. G.; Chen, W.; Wong, M. W.; Andres, J. L.; Head-Gordon, M.; Replogle, E. S.; Pople, J. A. *Gaussian 98*; Gaussian, Inc.: Pittsburgh, PA, 1998.

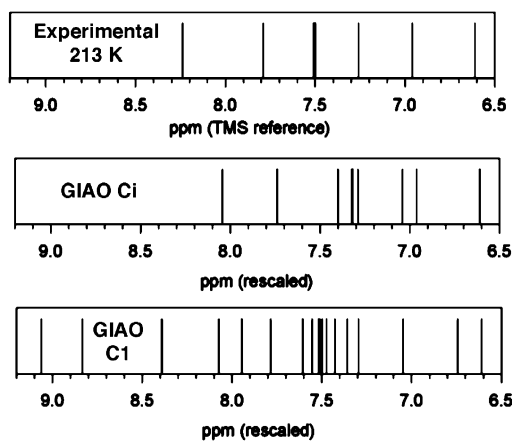(27) Forsyth, D. A.; Sebag, A. B. *J. Am. Chem. Soc.* **1997**, *119*, 9483−9494.

Figure 4. Bar graphs of experimental and GIAO chemical shifts of the aromatic (*ortho*- and *para*-) hydrogens of peroxide **2**. The positions of calculated shifts for the C_i and C_1 isomers were scaled relative to the higher field experimental signal.
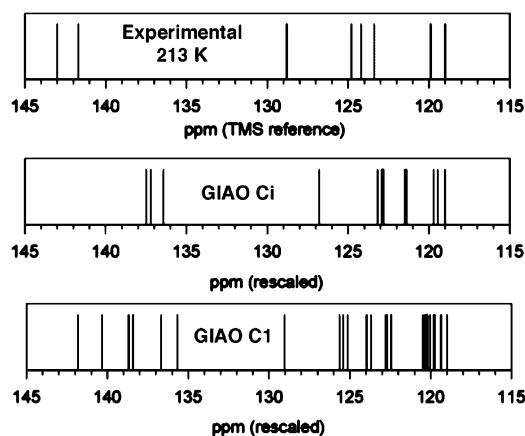

Figure 5. Bar graphs of experimental and GIAO chemical shifts of the aromatic (*ipso*-, *ortho*-, and *para*-) carbons of peroxide **2**. The positions of calculated shifts for the C_i and C_1 isomers were scaled relative to the higher field experimental signal.
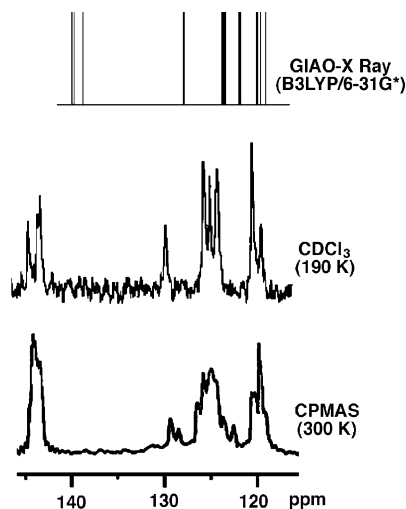

Figure 6. ^{13}C NMR signals corresponding to the *ipso* (143−145 ppm)-, *ortho* (122−130 ppm)-, and *para* (116−121 ppm)-hydrogens of **2**. Measurements in the solid state (CPMAS) were carried out at 300 K and in CDCl$_3$ at 190 K. The chemical shift dispersion of the GIAO model is smaller than that of the experimental one. See text for details.

those of the model trityl peroxide. While *ortho*- and *para*-^{1}H signals in the model trityl peroxide are isochronous,[28] the *tert*-butyl groups in **2** cause them to have a chemical shift difference

$\Delta\delta = 0.23$ ppm. Similarly, the *ipso*- and *para*-^{13}C signals of **2** and trityl peroxide have a $\Delta\delta = 23.3$ ppm and $\Delta\delta = 17.6$ ppm, respectively, making greater the signals of the simpler model to resonate 5.7 ppm closer. Thus, it seems reasonable that removal of the *tert*-butyl groups should result in a smaller chemical shift dispersion of the aromatic signals of the calculated spectrum. With that in mind, and recognizing that the assignments should be based more on a qualitative pattern matching that includes the total number of signals and the signal distribution rather than an accurate reproduction of signal positions, we propose that the spectrum calculated for the C_i isomer corresponds to the experimental one (support for this assignment by 2D TOCSY is discussed below). Not only is the C_1 structure predicted to have more signals than the C_i isomer, but the dispersion of signals both on ^{1}H and on ^{13}C spectra are significantly greater, in disagreement with expectations from the removal of the *tert*-butyl groups.

Inclusion of the solid-state ^{13}C CPMAS NMR spectrum in our analysis (Figure 6) supports the suggested assignment of the solution structure as that of the C_i isomer. From 12 aromatic carbon (*ipso*-, *ortho*-, and *para*-) signals in the calculated C_i spectrum, three sets are clearly distinguished in solution at low temperature and in the solid state at 300 K. Groups of signals centered at 139, 124, and 119 ppm in the calculated spectrum correspond to the *ipso*-, *ortho*-, and *para*- carbons, respectively. The experimental spectra measured in solution and in crystals have the same pattern with signals for *ipso*-, *ortho*-, and *para*-carbons centered at 144, 125, and 120 ppm. In agreement with the experimental and calculated ^{1}H NMR spectra, and consistent with field effects from the peroxide oxygen lone pairs and the aromatic π-systems, the *ortho*-carbons display the greatest chemical shift dispersion with a $\Delta\delta \approx 6$ ppm (Figure 6). One carbon is very deshielded ($\delta = 130$ ppm) and two others are shielded ($\delta = 122$ ppm) as compared to the rest which are centered at 125 ppm.[29]

Given the reasonable agreement between solution, solid-state CPMAS, and calculated ^{13}C spectra, the assignment of all of the hydrogen resonances in solution should be qualitatively reliable. A correlation between experimental and calculated *ortho* ^{1}H shifts is shown in Figure 7. Assignments in the calculated spectrum are based on the labels used in Scheme 1 and Figure 7 with aromatic rings labeled from Ar1 to Ar3 and the diastereotopic *ortho*-hydrogens identified by the labels "i" (in) and "o" (out), depending on their relation with respect to the internal peroxide bond. Although the calculated chemical shift dispersion of $\Delta\delta \approx 1.44$ ppm is smaller than the experimental one at $\Delta\delta \approx 1.67$ ppm, the agreement between the experimental (top) and calculated (bottom) *ortho*-signals is excellent. The calculation indicates that all of the "in" hydrogens (R3i, R1i, and R2i, shown in red) are deshielded as compared to the "out" hydrogens (shown in blue, Figure 7). The suggested assignment was also supported by results from a TOCSY (total correlation spectroscopy)[30] experiment, shown with horizontal bars in Figure 7. Cross-peaks between the two *ortho*-hydrogens

(28) (a) Henry-Ryan, H.; Tidwell, T. T. *J. Phys. Org. Chem.* **2003**, *16*, 559−563. (b) Branchaud, B. P. *J. Org. Chem.* **1983**, *48*, 3538−3544.
(29) The ^{13}C CPMAS NMR spectrum of **2** reveals two molecules per asymmetric unit from the doubling of the methane (94 and 95 ppm), *ortho*- (127 and 129 ppm), and other signals.
(30) Clean correlations between the two *ortho*, each of the two *ortho*-, and the *para*-hydrogens of each nonequivalent aryl ring were observed. Please see the Supporting Information for a copy of the 2D TOCSY spectrum.
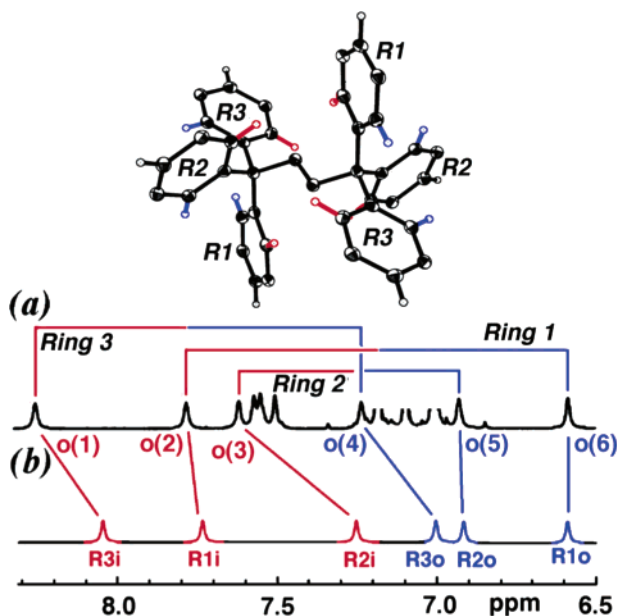
Figure 7. Correlation between (a) experimental chemical shifts for the *ortho*-signals of **2** at 193 K, and (b) calculated shifts normalized to the *ortho*-signal at 6.60 ppm (5 Hz line width). Horizontal lines indicate signals belonging to the same ring as determined by 2D TOCSY. Ring numbers are defined in the ORTEP diagram of peroxide **2** shown above with *tert*-butyl groups replaced by H.
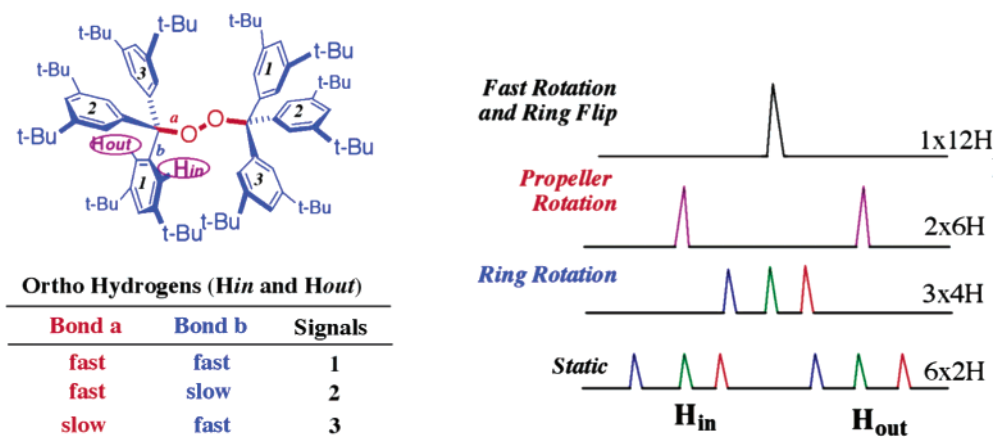
on a given ring correlate in a perfect pairwise manner with the upfield and downfield hydrogen signals, as predicted by the "in" and "out" assignments. Thus, with confidence gained by the relative shielding values calculated with the GIAO method and the long-range correlation of the TOCSY experiments, we assign signals o(1) and o(4) to Ar3i and Ar3o, the "in" and "out" *ortho*-hydrogens of ring 3, signals o(2) and o(6) to Ar1i and Ar1o (ring 1), and signals o(3) and o(5) to Ar2i and Ar2o (ring 2).

Coalescence Patterns. Knowing that the chemical shift dispersion of the *ortho*-hydrogens is determined by the position of the aromatic rings (Ar1−Ar3) and their orientation with respect to the peroxide group (Hin and Hout), we can analyze and simulate the ^{1}H NMR coalescence patterns in terms of various possible dynamic processes. In principle, each *ortho*-hydrogen can exchange with any one of the other five by rotation about either or both the C−O and the C−aryl bonds, which are labeled "a" and "b" in Scheme 3. With reference to the scheme, a mechanism involving fast rotation about the C−O and C−aryl

bonds will lead to collapse of all *ortho*-signals into a single, time-averaged resonance, as shown on the top trace. This process leads to the observation of a single "residual isomer" by ^{1}H NMR spectroscopy, and in the case of compound **2** it occurs at temperatures above 100 °C. A hypothetical dynamic process involving fast rotation about all of the bonds "b" with slow motion about the two bonds "a" would lead to the exchange of Hin and Hout resonances without altering the identity of the three aromatic rings. This mechanism would result in the collapse of signals in a pairwise fashion, giving rise to three singlets. It is clear from the results in Figure 3 and the analysis in Scheme 3 that simple rotation of the three aryl rings is not the main mechanism for the first coalescence process in peroxide **2**. In fact, it is well known that ring rotation in congested trityl derivatives occurs in a correlated fashion, leading to the enantiomerization of the axially chiral trityl groups (see below). The first coalescence of the *ortho*-signals from six to two at ca. 240 K requires exchange between the *ortho*-hydrogens in rings Ar1, Ar2, and Ar3, without losing their Hin and Hout identities. The most important difference between the idealized behavior shown in Scheme 3 and the experimental results in Figure 3 is the line-width of the two collapsed signals. Before reaching a condition where two sharp singlets can be observed, the experimental spectrum evolves from having two very broad lines into the single line that reflects fast exchange between all of the aromatic *ortho*-hydrogens. This observation is consistent with an activation barrier for a mechanism that exchanges the "in" and "out" hydrogens that is relatively close to that of the crankshaft mechanism. On the basis of this qualitative analysis and with the assignments shown in Figure 7, we carried out a detailed line-shape analysis to simulate the dynamic behavior of peroxide **2**.[31]

Although solvent interference obscures some regions of the experimental spectra, reasonably good simulations were obtained in the intermediate exchange regime with a dynamic model that considers initial rotation of the trityl groups about the "a" bonds, which is subsequently accompanied by a slower rotation about the "b" bonds (Figure 8). Data acquired between 193 and 243 K were simulated by exchanging the three "in" and the three "out" hydrogens with rate constants between 10 and 50 s^{-1}. As indicated in the figure, simulation of spectra acquired at $T \geq$ 253 K required the exchange of the "in" and "out" hydrogens with rate constants that are about half as large. An Eyring plot

Scheme 3

Ortho Hydrogens (H*in* and H*out*)

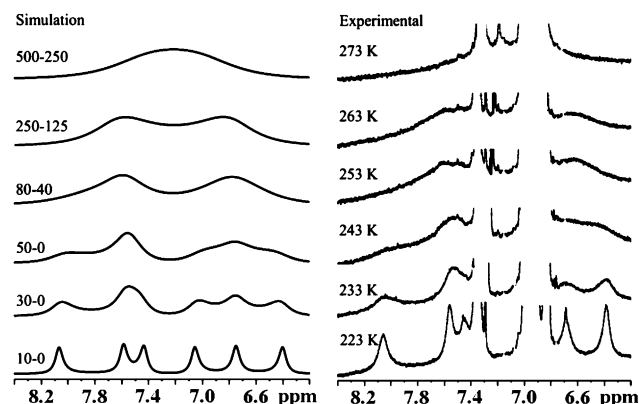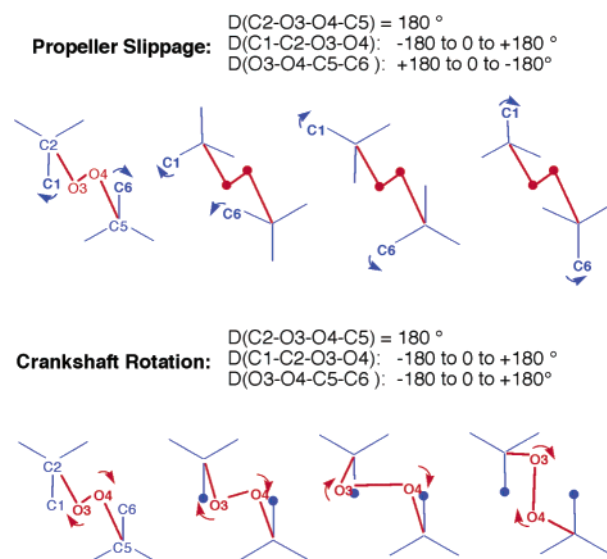| Bond a	Bond b	Signals
fast	fast	1
fast	slow	2
slow	fast	3
slow	slow	6

Figure 8. Aromatic region of the simulated and experimental ^{1}H NMR spectra of peroxide **2** at temperatures of intermediate exchange. The simulated spectra assume exchange between the three "in" and the three "out" *ortho*-hydrogens by rotation of the "a-bond" at a rate (in Hz) given by the first number, and rotation of the aryl groups by rotation of the "b-bond" at a rate (in Hz) given by the second number.

built with the rate constants for rotation of the "a" bonds within the temperature range from 192 to 350 K revealed an activation enthalpy of 8.7 kcal/mol and an entropy of −14.7 cal/(mol K). Unfortunately, it is not possible to determine activation parameters for the dynamic process that exchanges the identity of the "in" and "out" hydrogens.

Molecular Mechanics Calculations of Propeller Slippage and Crankshaft Motion. In search of computational support to help distinguish between simple "a"-bond rotation and the suggested crankshaft mechanism, we carried out molecular mechanics calculations to estimate their respective steric energy barriers. Molecular mechanics calculations were carried out with the MM+ force field of the program HyperChem using the coordinates of the X-ray structure as an input and varying the values of one or two dihedral angles while allowing the rest of the structure to relax. To calculate the energy barriers resulting from trityl group slippage and crankshaft motion, we formulated the structure of **2** as a system with three axes of rotation and four rotors. The axes of rotation are given by the C(2)−O(3), O(3)−O(4), and O(4)−C(5) bonds, while the four rotors are given by the adjacent atoms C(2)−O(3)−O(4)−C(5), as illustrated in Scheme 4. It should be noted that the bulky nature of the two trityl groups causes the peroxide dioxygen to remain close to a trans configuration at all times. As illustrated in Scheme 4, calculations aimed at modeling the slippage of the two trityl groups past each other were carried out by driving the C(1)−C(2)−O(3)−O(4) and O(3)−O(4)−C(5)−C(6) dihedral angles in opposite directions while the C(2)−O(3)−O(4)−C(5) dihedral of the peroxide group was kept anti at 180°. Kinematically, this procedure assumes a reference frame given by a static peroxide group and allows the two trityl groups to rotate past each other. It resulted in a barrier of 25 kcal/mol.

The crankshaft motion of the four-rotor system is described by correlated rotation about three adjacent dihedrals angles defined by six adjacent atoms. The end-rotors {C(2) and C(5)} remain stationary relative to each other, while the central ones {O(3) and O(4)} experience a circular motion. Crankshaft motion is described by concerted rotation of dihedrals C(1)−C(2)−O(3)−O(4) and O(3)−O(4)−C(5)−C(6) (shown from

(31) Spectral simulations were carried out with the following program: *g-NMR v. 5.0*; Adept Scientific, Inc.: Bethesda, MD.

Scheme 4

180° to 0° in Scheme 4). This motion preserves the dihedral angle C(2)−O(3)−O(4)−C(5) close to 180°, spontaneously maintaining the peroxide in the trans configuration. From a kinematic perspective, crankshaft rotation occurs in a reference frame defined by a constant position of the two trityl groups across the peroxide bond. The two aryl groups attached by C1 and C6 maintain their "anti relation", while the internal oxygen atoms rotate. One of the most interesting qualities of this motion in the case of peroxide **2** is that the molecular center of inversion present in the meso structure may be retained along the entire trajectory.

In agreement with the ^{1}H NMR simulations, a crankshaft trajectory exchanges the magnetic environment of *ortho*-hydrogens corresponding to the three nonequivalent rings while conserving their "in" and "out" identity. Given the viscosity of the solvent at low temperature, the difference between the MM+ calculated barrier (6.7 kcal/mol) and the experimental estimate (ca. 8.7 kcal/mol) is excellent and strongly supportive of a crankshaft mechanism rather than slippage of the bulky trityl groups. The crankshaft rotation has a period of 120° (Figure 9) and interconverts the three aryl groups while maintaining a meso (C_i) structure. The only structural change for site exchange to happen is a small reorientation of the aromatic planes without changing the absolute configuration of the chiral axis. The identities of the aromatic rings evolve from Ar1 → Ar3 → Ar2
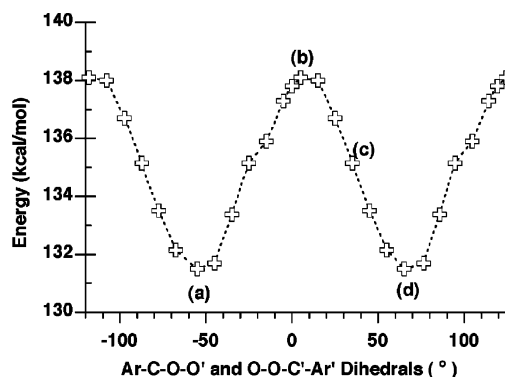

Figure 9. Rotational profile for the crankshaft motion of peroxide **2** calculated by molecular mechanics (MM+). The structures corresponding to points a−d are illustrated in Figure 10.

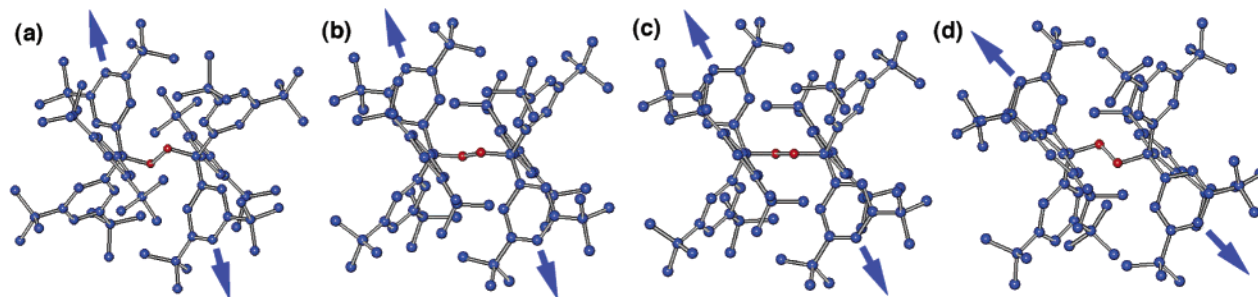**Figure 10.** Crankshaft motion in peroxide **2** illustrated with four structures with $Ar_1-C-O-O'$ and $O-O'-C'-Ar_1'$ dihedrals, of (a) $-55°$ and $55°$, (b) $13°$ and $-13°$, (c) $27°$ and $-27°$, and (d) $65°$ and $-65°$. The arrows along the 1,4-axis of two aryl groups related by the center of symmetry reveal the relatively minor reorientation of the aryl groups as the peroxide undergoes the crankshaft rotation. The anti conformation of the peroxide and the center of inversion of the molecule are maintained through the rotation. Structures labeled (a) and (d) are energy minima related by symmetry.

when crankshaft motion occurs in one sense, and from Ar1 → Ar2 → Ar3 when it occurs in the other. As the aryl groups sequentially transform into each other, the dihedral angles of their aromatic planes vary from 44.2° for Ar1 to 33.2° for Ar2 and 66.3° for Ar3. These changes are illustrated by the structures shown in Figure 10, which correspond to the points indicated by (a)−(d) along the potential shown in Figure 9. Small changes in the direction of the two trityl groups and in the orientation of the planes of all of the aryl substituents can be appreciated. Interestingly, this observation is consistent with the exchange between the rotary and the to-and-fro periodic motion expected in a crankshaft mechanism.

Energy barriers of 25 and 6.7 kcal/mol for slippage and crankshaft mechanisms strongly support the latter. However, changes in line shape as a function of temperature suggest that exchange trajectories involving rotation about the aryl−methane "b" bonds have only slightly higher barriers than the crankshaft motion. Therefore, in search of a more detailed picture of the dynamics of peroxide **2**, we decided to explore rotations about aryl−methane "b" bonds along trajectories similar to those described by Kurland[32] and Mislow[4] for the axial enantiomerization of triarylmethanes by the so-called "ring-flipping" mechanisms. In the case of peroxide **2**, enantiomerization of a single trityl group would lead to formation of the C_2 (or C_1) diastereomer, which is not observed under the conditions or our measurements but may occur as a short-lived transient along exchange trajectories. Double enantiomerization would preserve the meso structure.

The definition of ring flipping suggested by Kurland[32] involves reorientation of a ring by going through structures where the plane of the aromatic ring is perpendicular to the reference plane formed by the three *ipso*-carbons (Scheme 5). By that model, enantiomerization of the trityl group may occur by zero, one, two, or three ring flips. Notably, ring flipping as defined by this convention does not exchange the "in" and "out" identity of the *ortho*-hydrogens, but only the helical chirality of the trityl derivative. In fact, it is "nonflipping" rings rotating in the opposite direction, which are parallel to the same reference plane in the transition state, that will exchange the "in" and "out" identity of the *ortho*-hydrogens. Thus, while a zero ring flip mechanism exchanges the "in" and "out" hydrogens in all three rings, a three ring flip does not exchange any one. As shown in Scheme 5, we will refer to processes that exchange the planar diastereotopicity of these hydrogens as "ring rotations".

To estimate the barriers of ring flipping processes in peroxide **2**, we first analyzed hydroperoxide structure **3** (Scheme 5, X =

Scheme 5
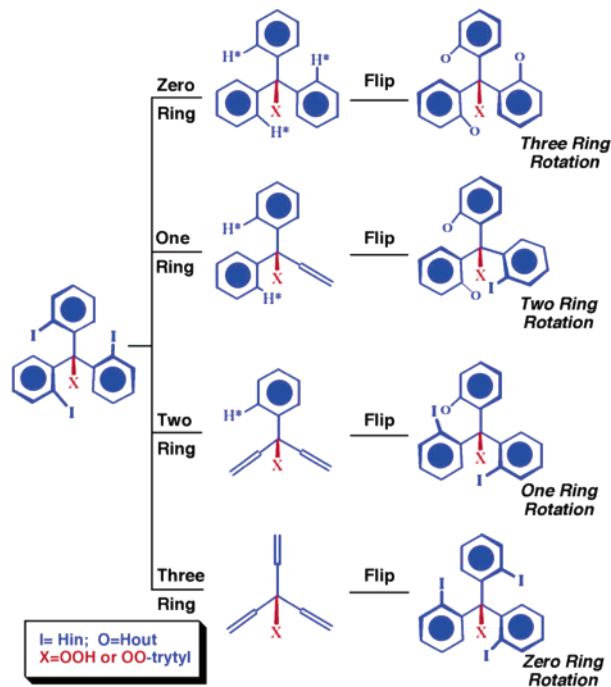
OOH). The structure of **3** with the six meta *tert*-butyl groups was obtained from the X-ray coordinates of **2**. The relative energies of transition states models with zero, one, two and three ring flips were obtained by setting the dihedral angles of each ring to values of 0° (no flip) or 90° (flip) with respect to the plane formed by three *ipso*-carbons. The structure involving a zero ring flip was the most unfavorable by ca. 42 kcal/mol. Structures involving one and three ring flips were close to each other but unfavorable by ca. 10 and 12 kcal/mol, respectively. According to the MM+ calculations, the most likely pathway for the enantiomerization of hydroperoxide **3** would be through two ring flip trajectories, which are only 2.5 kcal/mol above its minimum. The two ring flip transition state is strongly favored because it avoids the severe steric repulsion that would occur between the *tert*-butyl groups of adjacent rings. While actual enantiomerization trajectories are likely to deviate from a rigorous 0°, 0°, 90° structure, it is expected that these simple models will reflect the relative energetics of the transition state.

Thus, assuming that enantiomerization of peroxide **2** would occur by similar two ring flip processes, we investigated various

(32) Kurland, R. J.; Schuster, I. I.; Colter, A. K. *J. Am. Chem. Soc.* **1965**, *87*, 2279−2281.

structures that would represent the enantiomerization of only one or both propellers. Calculations were carried out by driving the dihedral angles of the flipping and nonflipping phenyl rings by 10–15° increments until they reached the desired values of 0° or 90°, respectively, while the rest of the structure was minimized. The transition states obtained in this manner for single and double enantiomerizations were 8.5 and 9.5 kcal/mol, respectively. Notably, these are only 1.8 and 2.8 kcal/mol higher than the barrier for crankshaft motion. When double enantiomerizations were considered, there were nine nonequivalent transition state models depending on which of the aryl groups adopted the flipping and nonflipping positions. The lowest energy structure was obtained when the flipping rings were Ar1 and Ar3 in one propeller and Ar1 and Ar2 (Scheme 3) in the other, suggesting a strongly correlated motion. Searching for experimental information to test this model, we explored the use of 2D-exchange spectroscopy (2D-EXSY). Under favorable circumstances, 2D-EXSY experiments are ideally suited for the analysis of systems with several nuclei concurrently exchanging among various positions.[33] Dynamic information is derived from the exchange that takes place as nuclei that start at a particular site carry their magnetization to new ones as a function of mixing times, allowing for a direct determination of specific exchange trajectories and rate constants. However, as the 2D-EXSY pulse sequence is identical to that employed in 2D-NOESY experiments, complications arise when dynamic exchange and magnetization transfer by NOE occur concurrently. For rigid molecules at very low temperatures in viscous solvents, magnetization transfer occurs very efficiently by spin diffusion. In fact, cross-peaks observed in experiments run with peroxide **2** suggested strong spin diffusion, which prevented the analysis of possible exchange trajectories.

Concluding Remarks

Crankshaft motions have been previously suggested within the context of conformational dynamics to account for the low-frequency relaxation dynamics of solid-state polymers[34] and proteins,[35,36] and for the dynamic disorder in crystals of *trans*-stilbenes and *trans*-azobenzenes.[37] In the case of *trans*-stilbene,
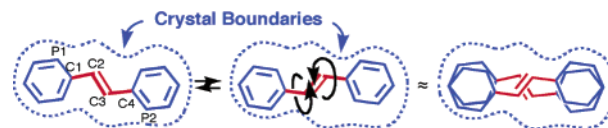

Figure 11. Reorientations of the double bond by a crankshaft motion have been proposed to account for the dynamic disorder responsible for the unusually short ethylene bonds in crystalline *trans*-stilbenes. The crankshaft rotation of C_2 and C_3 is accommodated by a small in-plane reorientation, but without flipping the phenyl groups (shown at right).

crankshaft rotation (also referred to as bicycle pedal motion) involves the rotary motion of ethylene carbons, C2 and C3, by simultaneous rotation about the dihedrals defined by $P_1-C_1-C_2-C_3$ and $C_2-C_3-C_4-P_2$, while the alkene bond between C2 and C3 remains *trans* at all times (Figure 11).

While crankshaft rotation in solids is defined by the reference frame provided by the bulk material, the rotary motion of the two oxygen atoms in bis-[tri-(3,5-di-*tert*-butyl)-phenylmethyl]-peroxide **2** can be defined by a reference frame provided by the position of the two trityl groups which are unable to pass each other due to the internal friction experienced by the bulky trityl groups. Although many different exchange trajectories can be envisioned, simple molecular mechanics indicates that crankshaft motion is more likely than random propeller rotation. We believe that volume-conserving motions, commonly postulated in polymers, biomolecules, and crystals, may prove important in the construction of solids engineered to support fast molecular motion. The preparation and analysis of other systems based on triarylmethanes that are expected to display rapid dynamics in solution and in crystals are currently in progress in our group.

Supporting Information Available: Crystallographic information file (CIF) of peroxide **2**. Tables with calculated and experimental chemical shift NMR data, VT ^1H NMR data in toluene-d_8 and CDCl$_3$, 2D TOCSY of peroxide **2** in toluene-d_8 at 193 K, and ORTEP figures and stereoviews illustrating the two molecules of peroxide **2**. This material is available free of charge via the Internet at http://pubs.acs.org.

JA046987C

(33) (a) Perrin, C. L.; Dwyer, T. J. *Chem. Rev.* **1990**, *90*, 935–967. (b) Macura, S.; Westler, W. M.; Markley, J. L. *Methods Enzymol.* **1994**, *239*, 106–144. (c) Jeener, J.; Meier, B. H.; Bachmann, P.; Ernst, R. R. *J. Chem. Phys.* **1979**, *71*, 4546–4553.

(34) (a) David, L.; Girard, C.; Dolmazon, R.; Albrand, M.; Etienne, S. *Macromolecules* **1996**, *29*, 8343–8348. (b) Hikmet, R. A. M.; Broer, D. J. P. *Polymer* **1991**, *32*, 1627–1632. (c) Gurler, M. T.; Crabb, C. C.; Dahlin, D. M.; Kovac, J. *Macromolecules* **1983**, *16*, 398–403. (d) Boyd, R. H.; Breitling, S. M. *Macromolecules* **1974**, *7*, 855–862. (e) Jones, A. A.; Stockmayer, W. H. *J. Polym. Sci., Polym. Phys. Ed.* **1977**, *15*, 847–861.

(35) (a) Demene, H.; Sugar, I. P. *J. Phys. Chem. A* **1999**, *103*, 4664–4672. (b) Shin, J.-M.; Oh, W. S. *J. Phys. Chem. B* **1998**, *102*, 6405–6412.

(36) For studies addressing the role of crankshaft-type motions in proteins, see: (a) Warshel, A. *Nature* **1976**, *260*, 679–683. (b) Cordfunke, R.; Kort, R.; Pierik, A.; Gobets, B.; Koomen, G.-J.; Verhoeven, J. W.; Hellingwerf, K. J. *Proc. Natl. Acad. Sci. U.S.A.* **1998**, *95*, 7396–7401.

(37) (a) Galli, S.; Mercandelli, P.; Sironi, A. *J. Am. Chem. Soc.* **1999**, *121*, 3767–3772. (b) Harada, J.; Ogawa, K.; Tomoda, S. *Acta Crystallogr.* **1997**, *B53*, 662–672. (c) Ogawa, K.; Sano, T.; Yoshimura, S.; Takeuchi, Y.; Toriumi, K. *J. Am. Chem. Soc.* **1992**, *114*, 1041–1051. (d) Saito, K.; Okada, M.; Akutsu, H.; Sorai, M. *Chem. Phys. Lett.* **2000**, *318*, 75–78. (e) McGeorge, G.; Harris, R. K.; Batsanov, A. S.; Churakov, A. V.; Chippendale, A. M.; Bullock, J. F.; Gan, Z. *J. Phys. Chem. A* **1998**, *102*, 3505–3513.